DOE/PC/91309--T7

MAR 09 1993

HIGH TEMPERATURE ALKALI CORROSION OF CERAMICS IN COAL GAS

DOE/PC/91309--T7

DE-FG22-91PC91309

DE93 011634

Quarterly Progress Report #6
for the Period
December 1, 1992 - February 28, 1993

Prepared by

G.R. Pickrell, T. Sun, and J.J. Brown

Center for Advanced Ceramic Materials
Virginia Polytechnic Institute
and State University
Blacksburg, VA 24061

Prepared for

Department of Energy
Pittsburgh Energy Technology Center
P.O. Box 10940
Pittsburgh, Pennsylvania 15236

February 24, 1992

MASTER

"U.S. DOE Patent Clearance is not required prior to the publication of this document."

DISTRIBUTION OF THIS DOCUMENT IS UNLIMITED

Summary of Current Report

The high temperature alkali corrosion kinetics of SiC have been systematically investigated from 950 to 1100°C at 0.63 vol% alkali vapor concentration. The corrosion rate in the presence of alkali is approximately 10^4 to 10^5 times faster than the oxidation rate of SiC in air. The activation energy associated with the alkali corrosion is 406 kJ/mol, indicating a highly temperature-dependent reaction rate. The rate-controlling step of the overall reaction is likely to be the dissolution of silica in the sodium silicate liquid, based on the oxygen diffusivity data.

DISCLAIMER

This report was prepared as an account of work sponsored by an agency of the United States Government. Neither the United States Government nor any agency thereof, nor any of their employees, makes any warranty, express or implied, or assumes any legal liability or responsibility for the accuracy, completeness, or usefulness of any information, apparatus, product, or process disclosed, or represents that its use would not infringe privately owned rights. Reference herein to any specific commercial product, process, or service by trade name, trademark, manufacturer, or otherwise does not necessarily constitute or imply its endorsement, recommendation, or favoring by the United States Government or any agency thereof. The views and opinions of authors expressed herein do not necessarily state or reflect those of the United States Government or any agency thereof.

Objective/Scope

High temperature alkali corrosion has been known to cause premature failure of ceramic components used in advanced high temperature coal combustion systems such as coal gasification and clean-up, coal fired gas turbines, and high efficiency heat engines. The objective of this research is to systematically evaluate the alkali corrosion resistance of the most commonly used structural ceramics including silicon carbide, silicon nitride, cordierite, mullite, alumina, aluminum titanate, zirconia, and fireclay glass. The study consists of identification of the alkali reaction products (phase equilibria) and the kinetics of the alkali reaction as a function of temperature and time.

Review of Alkali Corrosion on SiC

Molten salt corrosion of SiC has been studied as early as 1952 when Horn[1] investigated the corrosive effects of immersion of single crystal alpha-SiC in molten sodium carbonate at 1000°C and observed dislocation etch pitting. Amelincks et al[2] and Buchner et al[3] also looked at molten sodium carbonate corrosion of SiC. The former reported dislocation etch pitting at 1000°C and the latter reported complete dissolution at temperatures less than 900°C. McKee et al[4] studied both salt immersion and thin film depositions of sodium sulfate and sodium carbonate on beta-SiC and reported active corrosion by deep basic melts with carbon added. Tressler et al[5] studied the corrosion of reaction bonded and hot pressed SiC in mixtures of

sodium chloride and sodium sulfate at 1200°C. They found that SiC corroded rapidly provided the O^{2-} activity was sufficiently high. Becher[6] and Ferber et al[7] examined the reactions between SiC and slurry coatings of powdered coal combustion slags at 1200-1300°C. The former found faster corrosion in basic slags, but more strength reduction in acidic slags. The latter reported pitting and strength reduction for coal slurry coatings greater than 100 μm. Blachere et al[8] deposited thin films of sodium sulfate on CVD, single crystal and hot pressed SiC at 1000°C, noting that bubble formation, devitrification and cracking of the SiO_2 layer occurred. Jacobsob et al[9] studied the effects of thin film coatings of sodium sulfate and sodium carbonate on SiC at 1000°C and found that the acid attack was severe only in the presence of free carbon, but the basic attack led to severe pitting in all the materials studied. Jacobson[10] also used a burner rig at 4 atm and 1000°C seeded with 4 ppm Na to model the continuous deposition of sodium sulfate that is likely to occur in real systems. It was found that corrosive attack led to a 32% decrease in strength of SiC. Smialek et al[11] using thin films of sodium sulfate and sodium carbonate on sintered alpha-SiC noted a 13-49% reduction in strength depending upon the salt and the gaseous environment used, and concluded that pitting was the major factor in strength reduction.

The various results reported on the alkali corrosion of SiC are largely confined to phenomenological description, and there has been no systematic study of the high temperature alkali corrosion of SiC regarding the accelerated oxidation rate of SiC and the possible rate-controlling step in the presence of alkali vapors. Therefore, the present study concentrates on the kinetics of high temperature, gaseous alkali corrosion of SiC.

Experimental Procedure

The system from which alkali vapors were generated and transported to the reaction chamber during the alkali corrosion test is shown in Figure 1. The compressed air flowing into the system was filtered to remove CO_2 and moisture. The flow rate of the filtered compressed air was controlled by a flow meter and fixed at 200 ml/min. The filtered gas flowed over the alumina boat containing sodium nitrate in a mullite tube, picked up and transported the alkali vapors to the sample chamber at the center of the tube furnace, and exited the rear of the tube. A long mullite tube was used to allow the inlet side to be heated separately with a heating tape to 735°C. This allowed control of the temperature of the salt independently of the temperature of the furnace, and thus fixed the concentration of the salt at all testing temperatures.

The outlet tube was connected to a glass moisture collection chamber immersed in an ice bath to examine whether or not steam was present in the atmosphere. The flow rate was maintained at 200 ml/min through the glass chamber for 16 h during the corrosion test. There was no condensed water present in the collection chamber.

The boats were weighed before and after each run to determine the amount of weight loss of the sodium nitrate during the corrosion time interval. Figure 2 shows the weight loss of the salt as a function of time. The weight loss data follow a linear trend, indicating a constant alkali concentration throughout the reaction. The slope gives a linear weight loss of 0.26 g sodium nitrate per hour. Using data from the weight loss and the flow rate of the compressed air, the alkali vapor concentration

was calculated to be approximately 0.63 vol%. A summary of the experimental conditions is shown in Table I.

The thickness change of the SiC pellets exposed to the alkali containing atmosphere was measured using a micrometer after removal of the glassy layer by a 15 minute soak in HF solution, and the microstructure was examined using SEM.

Results and Discussion

(a) Parabolic Reactions

A plot of thickness squared of the corrosion product versus time is shown in Figure 3 for each reaction temperature according to the parabolic rate law, $x^2 = k_p t$, where x, k_p, and t represent the thickness of the sodium silicate glass, the rate constant, and the reaction time, respectively. The calculated rate constants at temperatures from 950 to 1100°C are listed in Table II. Figure 4 shows the Arrhenius plot of the reaction rate versus temperature according to the rate equation $k_p = k_0 \exp(-Q/RT)$. The reaction rate appears to be highly sensitive to temperature changes as manifested in the high activation energy (406 kJ/mol) calculated from the Arrhenius plot.

The effects of alkali on the corrosion of SiC can be demonstrated by comparing the oxidation rate of SiC in air with the alkali corrosion rate of SiC at the same temperature, as listed in Table II. Due to the sluggish oxidation at temperatures below 1200°C, the rate constants for the oxidation of SiC in air were extrapolated from the experimental data by Costello et al[12]. The data indicate that the corrosion rate of SiC

is significantly faster in the presence of alkali than in air, with a quotient of the two rate constants ranging from 3.04×10^4 at 950°C to 4.34×10^5 at 1100°C. The dramatic increase in the reaction rate is attributed to the high oxygen diffusivity in the sodium silicate glass when compared to the oxygen diffusivity in pure vitreous silica (Table II). The effect of alkali concentration on the corrosion rate can also be estimated knowing the rate constant k_p at a given concentration, since the rate constant is proportional to the concentration.

(b) Accelerated reactions

It should be pointed out that the above kinetic data were based on relatively short term alkali exposures. It was found that, however, an anomalous reaction occurred for longer exposure time at 1050°C. For reaction time longer than 15 h, the reaction rate becomes nonlinear and increases with time as shown in Figure 5. The glassy layer becomes progressively thicker with time up to about 15 hours. Examination of the reacted specimens shows that the alkali glass had flowed from the pellet surface onto the alumina holder, therefore changing the boundary conditions of the parabolic rate law. It is believed that the viscous flow of the glassy layer causes the increased corrosion rates for the longer time periods.

(c) Microstructure Analysis

Figure 6 shows the SEM micrographs of the fracture surface of the as received specimen and the surface of the SiC after a 24 h exposure at 1000°C in the alkali containing atmosphere (after removal of the glassy layer). The SiC was preferentially

attacked at the grain boundaries producing well defined grains as seen in these micrographs. Figure 7 reveals the interface cracking between the soda glass and the unreacted SiC after reaction at 1000°C. The interface cracking is likely to result from the thermal expansion mismatch between the soda glass and SiC during quenching. In all cases, the formation of a glassy layer is evident which supports a continuous dissolution-oxidation mechanism of the alkali enhanced oxidation of SiC.

(d) Rate-Controlling Step

The alkali corrosion of SiC is schematically shown in Figure 8. The formation of a sodium silicate glass at the reaction temperature provides a rapid transport of oxygen for the oxidation of SiC. The silica formed at the interface is then dissolved in the sodium silicate due to the continuous supply of alkali from the atmosphere. If the dissolution of the silica layer is fast relative to the diffusion of oxygen through the sodium silicate, the overall reaction rate is controlled by the diffusion rate of oxygen through the silicate layer. On the other hand, if the dissolution of the silica layer is relatively slow compared to the diffusion of oxygen through the silicate, the overall reaction rate is controlled by the dissolution rate of the silica layer in the silicate melt.

Assuming local equilibrium between the liquid phase and silica is achieved, the composition of the sodium silicate is likely to be $Na_2O \cdot 4SiO_2$ according to the Na_2O-SiO_2 phase diagram (Figure 9). The oxygen diffusivities in fused silica and sodium silicate glass ($Na_2O \cdot 4SiO_2$) are listed in Table II. As shown in Table II, the increase of oxygen diffusivity between pure silica and sodium silicate at all temperatures appears to be greater than the increase of the reaction rate when the oxidation of SiC in air

is compared with the oxidation of SiC in the presence of alkali. The activation energy of oxygen diffusion in the sodium silicate glass is only 186 kJ/mol, which is significantly less than the activation energy (406 kJ/mol) of the alkali reaction from the present study. The results suggest that the overall alkali reaction may be controlled by the dissolution of silica, instead of the oxygen diffusion, in the sodium silicate.

Summary

1. The alkali corrosion kinetics of SiC have been investigated from 950 to 1050 °C at 0.63 vol% alakli concentration.

2. The alkali corrosion rate of SiC was approximately 10^4-10^5 times the oxidation rate of SiC in air.

3. The activation energy is 406 kJ/mol from 950 to 1050°C.

4. Based on the oxygen diffusivity, the alkali corrosion rate of SiC is slower than expected, possibly controlled by the dissolution of silica in the silicate.

Table I. Experimental Condition

Alkali Concentration	:	0.63 vol%
Temperature	:	950-1100°C
Gas Flow Rate	:	200 mL/min
Time	:	1-115 h
No. Specimens/Exposure	:	4
Specimen Dimensions	:	0.2x0.2x0.5 cm
Glass Removal Procession	:	15 min. in HF solution

Table II. Corrosion Kinetics of SiC and Oxygen Diffusivity in Fused Silica and Sodium Silicate ($Na_2O \cdot 4SiO_2$)

	Rate Constant ($\mu m^2/h$)		Oxygen Diffusivity (cm^2/s)	
Temp (°C)	Alkali	Air	Silica	Silicate
950	12.3	4.1×10^{-4}	4.2×10^{-16}	1.0×10^{-9}
1000	75.8	7.3×10^{-4}	1.0×10^{-15}	2.0×10^{-9}
1050	390.0	1.2×10^{-3}	2.4×10^{-15}	4.0×10^{-9}
1100	890.0	2.1×10^{-3}	5.2×10^{-15}	7.0×10^{-9}
E_a (kJ/mol)	406	134-389	234	186
		Ref. 12	Ref. 14	Ref. 13

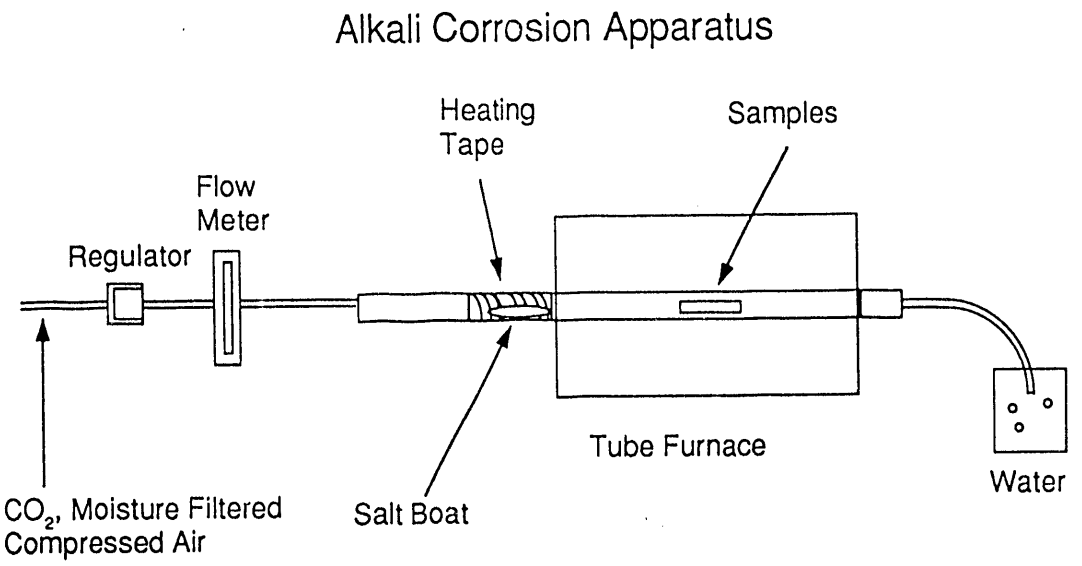

Figure 1. Schematic of alkali corrosion apparatus.

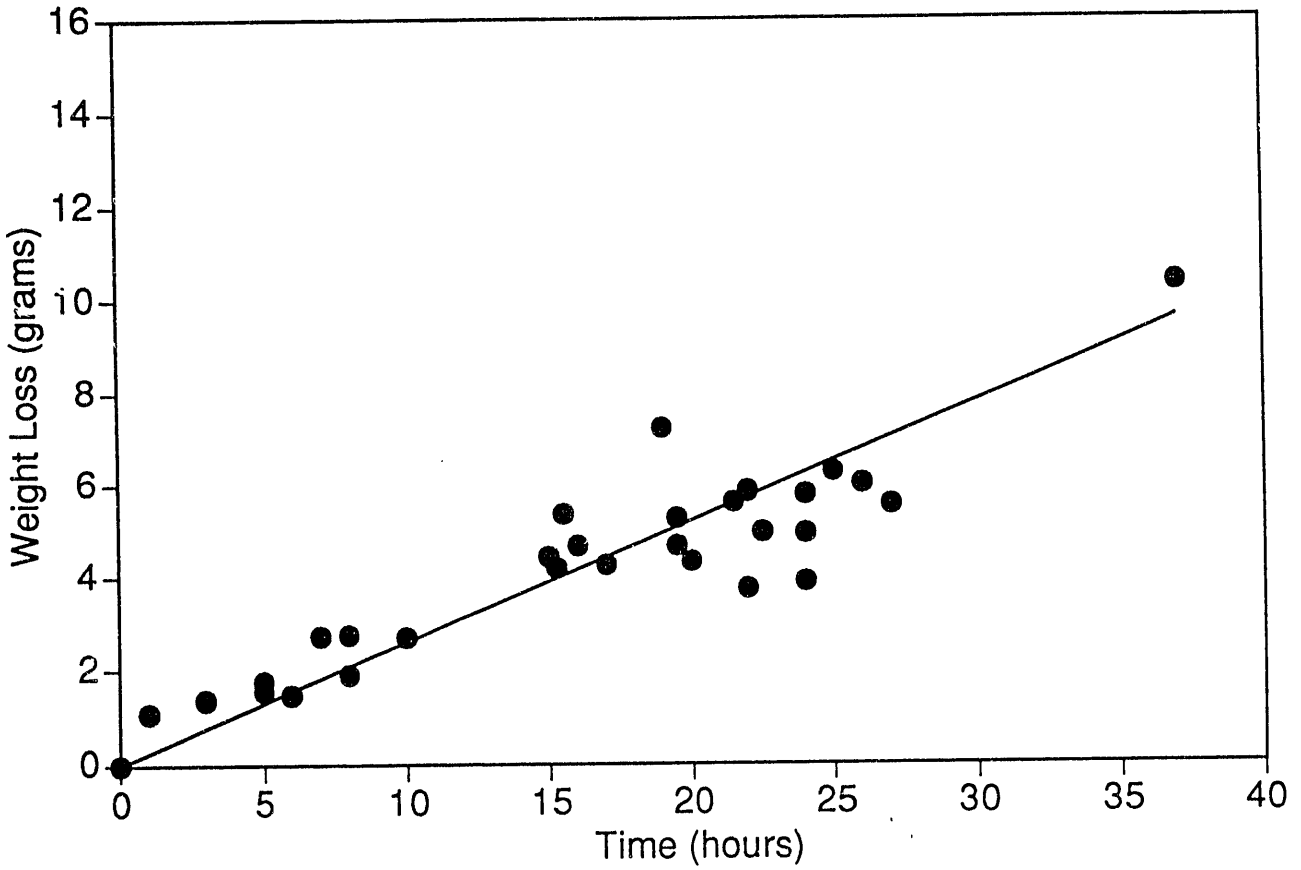

Figure 2. Weight loss of sodium nitrate versus time.

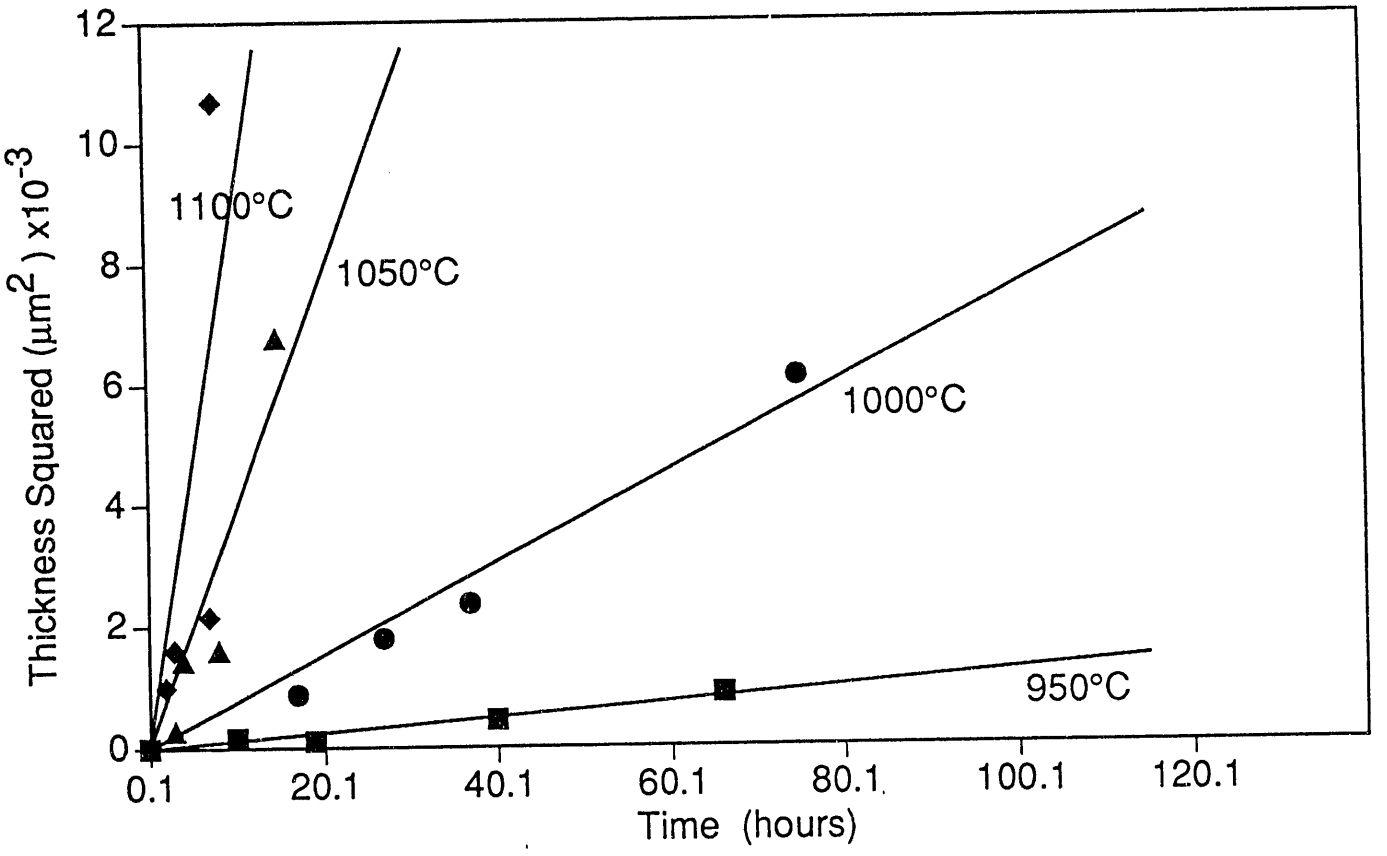

Figure 3. Thickness squared of the soda glass as a function of temperature and time.

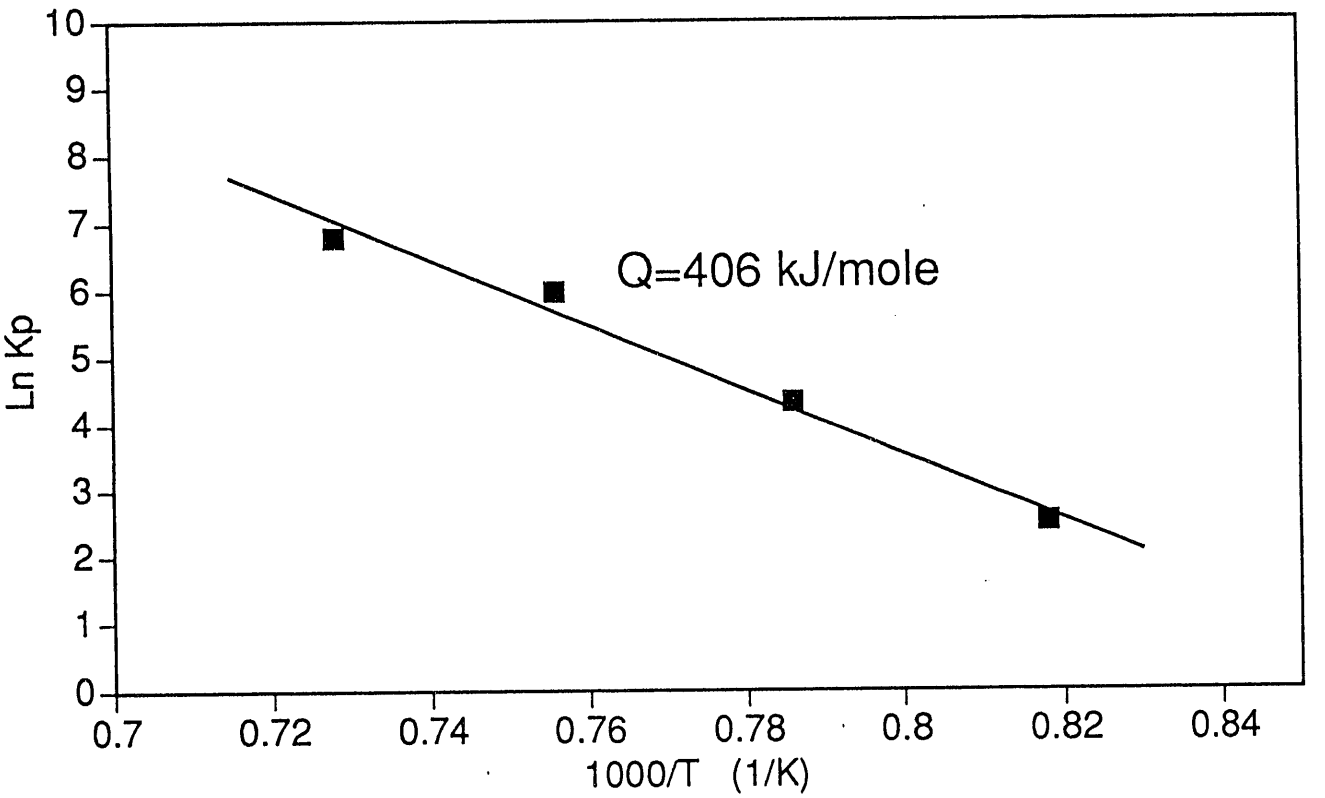

Figure 4. The Arrhenius plot of the alkali reaction rate versus temperature.

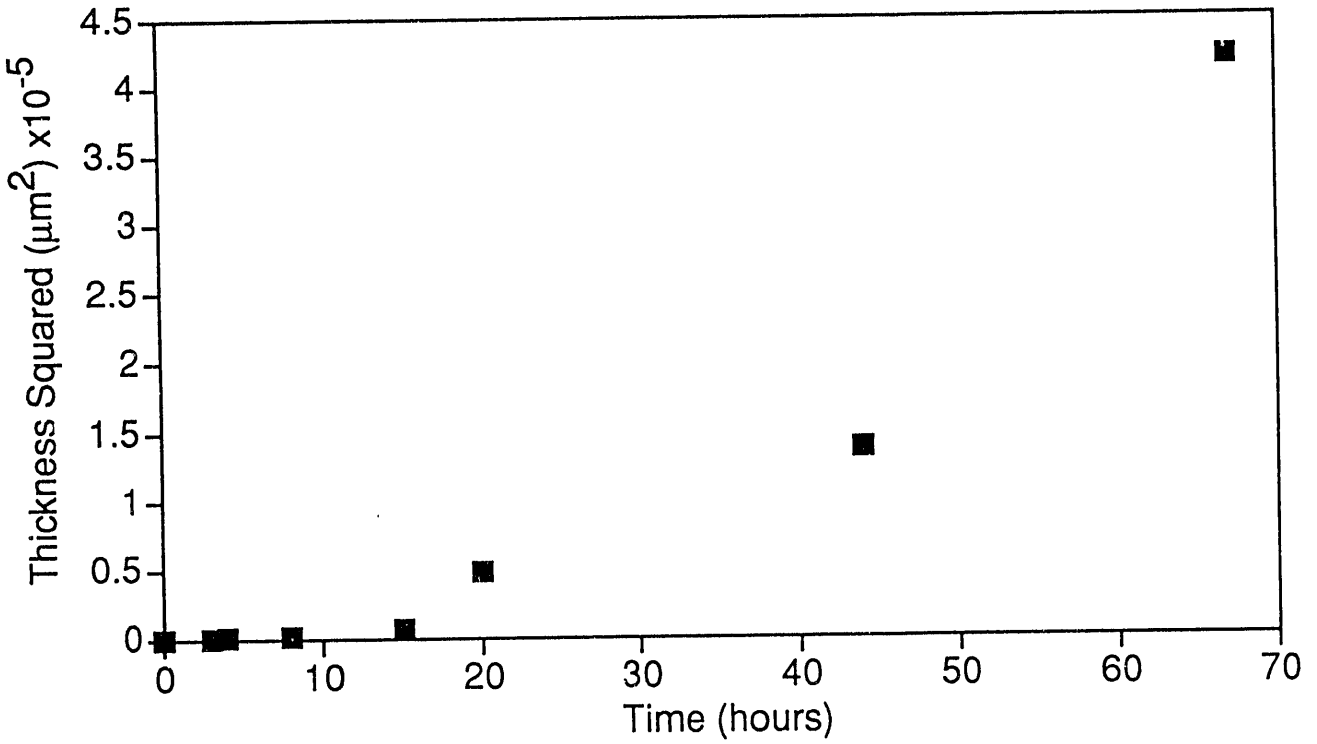

Figure 5. Thickness squared of the soda glass at 1050°C.

a.)

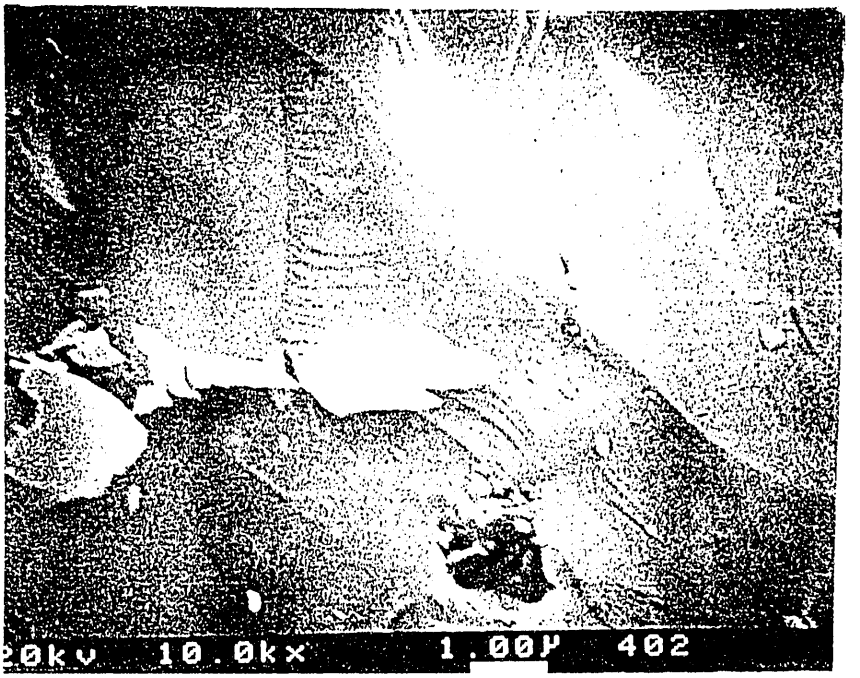

b.)

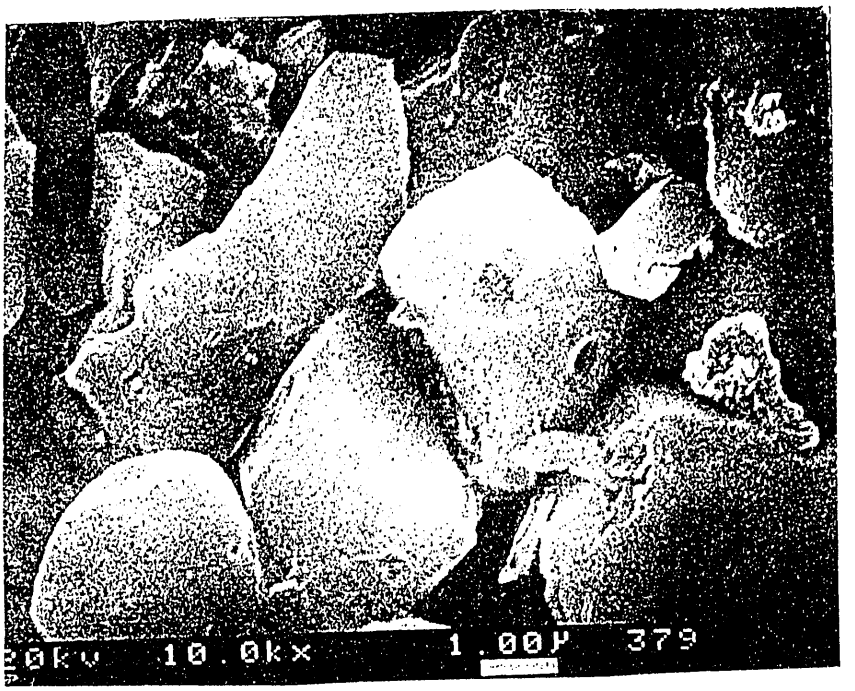

Figure 6. SEM micrographs of a.) fracture surface of as received SiC surface b.) 1000°C exposure in 0.63 vol% alkali atmosphere after removal of the glassy layer.

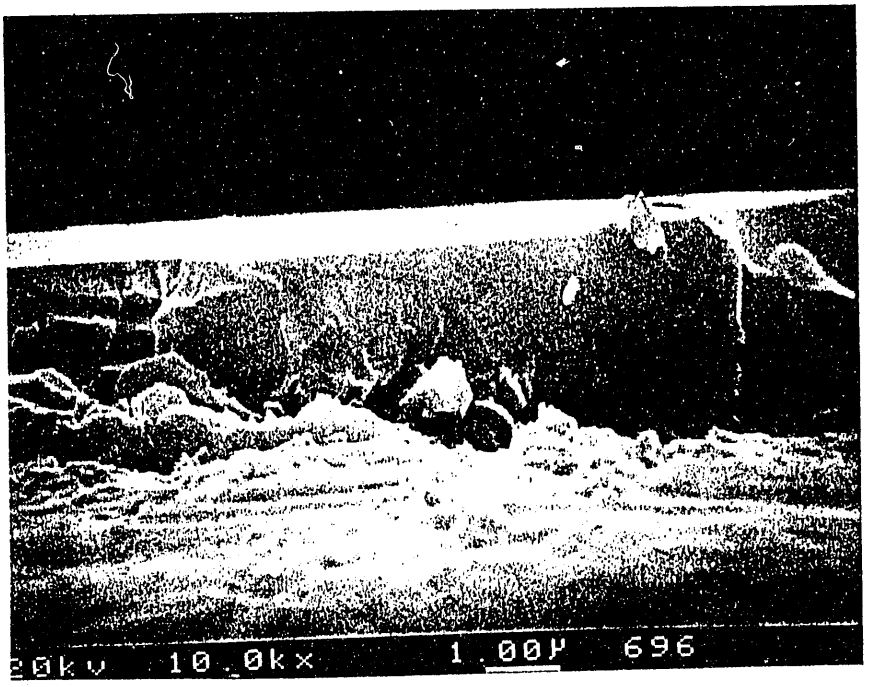

Figure 7. SEM micrograph of the glassy reaction layer formed on the SiC surface after exposure at 1000°C in 0.63 vol% alkali atmosphere.

Corrosion Process

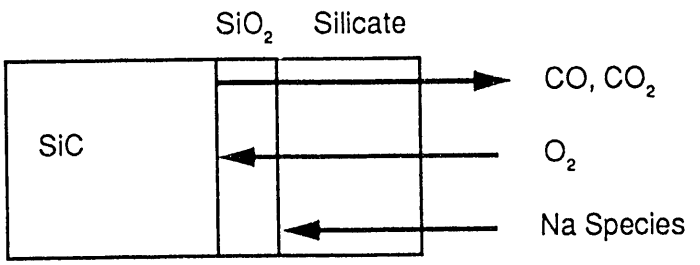

$$SiC + \tfrac{3}{2}O_2 \longrightarrow SiO_2 + CO$$

$$SiC + 2O_2 \longrightarrow SiO_2 + CO_2$$

$$SiO_2 + Na_2O \longrightarrow \text{Sodium Silicate}$$

Figure 8. Schematic of the alkali corrosion of SiC.

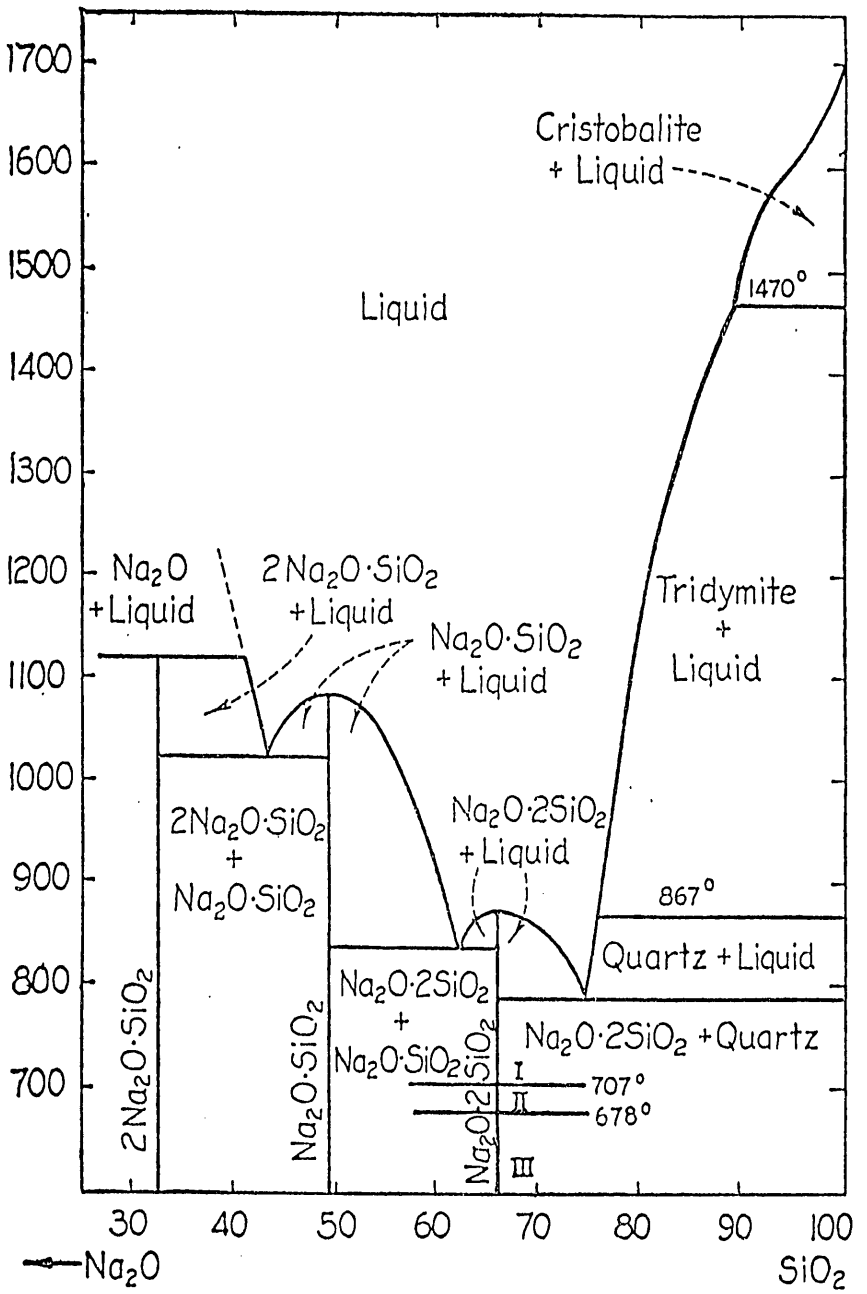

Figure 9. Phase diagram of the Na_2O-SiO_2 system.

REFERENCES

1. F.H. Horn "Screw Dislocations, Etch Figures, and Holes," Philos. Mag., 43, 1210-13 (1952)

2. S. Amelinckx, G. Strumane and W.W. Webb, "Dislocations in Silicon Carbide," J. Appl. Phys. 31, 1359-70 (1960)

3. E. Buchner and O. Rubisch, pp 428-34 in Silicon Carbide-1973. Edited by R.C. Marshall and J. W. Faust. University of South Carolina Press, Columbia, SC, 1974

4. D.W. McKee and D. Chatterji, "Corrosion of SiC in Gases and Alkaline Melts", J. Am. Ceram. Soc., 59 [9-10] 441-44 (1976)

5. R.E. Tressler, M.D. Meiser and T. Yonushonis, "Molten Salt Corrosion of SiC and Si_3N_4 Ceramics" J. Am. Ceram. Soc., 59 [5-6] 278-79 (1976)

6. P. Becher, "Strength Degradation in SiC and Si_3N_4 Ceramics by Exposure to Coal Slags at High Temperatures", J. Mater. Sci., 19, 2805-14 (1984)

7. M.K. Ferber, J. Ogle, V.J. Tennery and T. Henson, "Characterization of Corrosion Mechanisms Occurring in Sintered SiC Exposed to Basic Coal Slags", J. Am. Ceram. Soc. 68 [4] 191-197 (1985)

8. J.R. Blachere and F.S. Petit, "High Temperature Corrosion of Ceramics",DOE/ER/10915-3, 1984

9. N.S. Jacobson and J.S. Smialek, "Hot Corrosion of Sintered α-SiC", J. Am. Ceram. Soc., 68 [8] 432-39 (1985)

10. N.S. Jacobson, C.A. Stearns and J.L. Smialek, "Burner Rig Corrosion of Silicon Carbide at 1000°C", Adv. Ceram. Mater., 1 [2] 154-61 (1986)

11. J.L. Smialek and N.S. Jacobson, "Mechanism of Strength Degradation for Hot Corrosion of α-SiC", J. Am. Ceram. Soc., 69 [10]741-52 (1986)

12. J.A. Costello and R.E Tressler "Oxidation Kinetics of Hot-Pressed and Sintered α-SiC", J. Am. Ceram. Soc., 64 [6] 327-31 (1981)

13. Y. Oishi, R. Terai and H. Ueda, "Oxygen Diffusion in Liquid Silicates and Their Relation to Viscosity", pg 297-311 in Materials Science Research Volume 9: Mass Transport in Ceramics, 1975, edited by A.R. Cooper and A.H. Heuer

14. H. Schaeffer, "Silicon and Oxygen Diffusion in Oxide Glasses", pg 311-325 in Materials Science Research Volume 9: Mass Transport in Ceramics, 1975, edited by A.R. Cooper and A.H. Heuer

END

DATE
FILMED
5/19/93